UC Santa Barbara
UC Santa Barbara Previously Published Works

Title
Thermodynamic considerations in the stability of binary oxides for alternative gate dielectrics in complementary metal-oxide-semiconductors

Permalink
https://escholarship.org/uc/item/3k2710r7

Journal
Journal of Vacuum Science & Technology B, 22(2)

ISSN
1071-1023

Author
Stemmer, Susanne

Publication Date
2004-03-01

Peer reviewed

eScholarship.org Powered by the California Digital Library
University of California

Thermodynamic Considerations in the Stability of Binary Oxides for Alternative Gate Dielectrics in CMOS

Susanne Stemmer[a)]

Materials Department, University of California, Santa Barbara, CA 93106-5050

[a)] Electronic mail: stemmer@mrl.ucsb.edu

Abstract

A number of binary oxides have been predicted to be thermodynamically stable in contact with Si and are candidates to replace SiO_2 in CMOS. However, reactions leading to the formation of interfacial silicide, silicate or SiO_2 layers have been reported when these oxides are exposed to high temperatures during device processing. Different pathways have been proposed in the literature to explain these reactions. In this paper, a thermodynamic analysis of the proposed reactions is performed. The analysis includes gaseous species, because typical gate dielectrics are ultra-thin layers and diffusivities for species from the surrounding atmosphere, such as oxygen, may be high. Furthermore, nonstoichiometry of the high-*k* oxide, as may be resulting from nonequilibrium deposition processes or reducing atmospheres during processing is also considered. Studies are proposed to distinguish between possible reaction mechanisms. Finally guidelines for stable interfaces are presented.

I. Introduction

Due to the continuous decrease in feature size, silicon devices are approaching a number of fundamental limits. In particular, the gate oxide in modern complementary metal oxide semiconductor devices (CMOS) has reached atomic dimensions. When the thickness of the traditionally used gate dielectric materials, SiO_2 and Si-oxynitrides, falls below ~ 1 nm, leakage currents are excessive due to direct tunneling. Use of a different gate oxide with higher dielectric constant (k) reduces leakage currents as a greater physical thickness of the gate dielectric can be realized. Gate stacks are exposed to high temperature rapid thermal anneals during device fabrication, typically around 1000 °C. Therefore, an important consideration in the selection of an alternative gate dielectric is its thermal stability in contact with Si and the gate electrode, respectively. HUBBARD and SCHLOM evaluated the thermodynamic stability of a large set of binary oxides (MO_x) in contact with Si [1]. For example, ZrO_2 and HfO_2, two potential candidates to replace SiO_2 as the gate dielectric, were predicted to be thermodynamically stable in contact with Si up to ~ 1200 °C [1,2]. However, thermodynamic stability analysis considering only reactions between two stoichiometric solids appears to be insufficient for predicting stable heterointerfaces. Interfacial phases, such as silicides, SiO_2, and silicates, are often observed in real high-k dielectric gate stacks exposed to high temperatures [3-14], as schematically illustrated in Fig. 1.

Undesirable, low-k interfacial SiO_2 significantly increases the achievable equivalent oxide thickness, defined as the thickness of the high-k dielectric scaled by the ratio of its dielectric constant to that of SiO_2. The growth of high-k gate oxides thus becomes a challenging balance of employing sufficiently high O_2 partial pressures to completely oxidize the high-k material, however, without oxidizing the Si. Furthermore, during device processing, oxygen

present in the annealing atmosphere may diffuse through the ultrathin high-*k* oxide and react with Si.

Interfacial silicides form under reducing conditions [3-5,15,16], while silicate layers are often observed at interfaces between Si and rare-earth or related oxides. While the experimental conditions under which these layers form are relatively well understood, significant disparity exists in the literature with respect to the reactions causing the formation of interfacial layers, in particular the silicides [4-9,17,18].

The goal of this paper is to provide a thermodynamic basis of possible reaction pathways that have been proposed in literature. The analysis focuses on a few examples of binary oxides. Unless stated otherwise, the thermodynamic data were obtained from tables by BARIN [19]. Similar calculations can be carried out for other candidate oxides, as reliable thermodynamic data become available.

The paper is arranged as follows. In section II, conditions are presented under which interfacial SiO_2 forms during deposition or uncapped high-temperature anneals. In section III, a thermodynamic analysis is performed of silicide reactions that have been proposed in literature. Section IV treats possible origins of interfacial rare-earth silicates. Finally, guidelines for stable interfaces are presented.

II. Conditions for Interfacial SiO_2 Growth

a) Driving forces for SiO_2 formation during high-*k* oxide growth

If oxygen can be transported to the Si interface, either during processing or growth, a driving force for SiO_2 formation exists even for gate oxide materials that are thermodynamically stable in contact with silicon [2]:

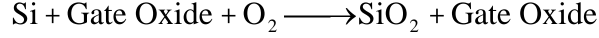

$$\text{Si} + \text{Gate Oxide} + \text{O}_2 \longrightarrow \text{SiO}_2 + \text{Gate Oxide}$$

$$\Delta G^\circ_{(1)} = -679\,\frac{\text{kJ}}{\text{mol}}, \quad (1)$$

where $\Delta G^\circ_{(1)}$ is the free energy change of the reaction between reactants and products, all taken to be in their standard state, proceeds in the direction indicated at a temperature of 1300 K.

Figure 2 shows the equilibrium O_2 partial pressure (p_{O_2}) for the formation of the binary oxides of Si, Zr and Hf, as a function of temperature. This figure shows that for all viable p_{O_2}'s during high-*k* growth, a driving force for SiO_2 formation exists. However, under conditions of low p_{O_2}'s and sufficiently high temperatures, SiO gas is known to desorb from **bare or SiO_2 covered silicon surfaces** [20-22], resulting in a clean (oxide free) Si surface. SiO desorption is described by the following equations

$$2\text{Si} + \text{O}_2 \rightarrow 2\text{SiO(g)} \quad (2a)$$

$$\text{Si} + \text{SiO}_2 \rightarrow 2\text{SiO(g)} \quad (2b)$$

The p_{O_2} and temperature ranges under which SiO_2 growth (eqn. (1)) and the competing SiO etching (eqn. (2a)) reaction occur for a **bare silicon wafer** have been determined experimentally [20-22] and are also shown in Fig. 2. The p_{O_2}'s and temperatures for clean Si are accessible during high-*k* oxide growth by physical vapor deposition. SiO_2 free growth surfaces are thus feasible. However, low p_{O_2}'s during growth may cause the high-*k* oxide to become oxygen-deficient, as will be discussed in detail in section III.

Figure 3 schematically summarizes the proposed reactions that could lead to SiO_2 or SiO formation during uncapped anneals of high-*k* dielectrics on Si. If the high-*k* oxide shows sufficient oxygen permeability, interfacial SiO_2 growth is expected if

- the p_{O_2} and temperature are in the range in which reaction (1) is favored over reaction (2) **or**
- the p_{O_2} and the temperature are in the range in which reaction (2) is favored **and** kinetic barriers exist for SiO formation (discussed in detail in section II c).

SiO_2 forms also in the second case, because the driving force for reaction (1) still exists, provided that the p_{O_2} is above the "SiO_2" stability line in Fig. 2. At a fixed temperature the minimum p_{O_2} at which SiO_2 forms beneath a high-*k* layer on Si would be expected to depend on the thickness and microstructure of the overlying high-*k* film. Next, these two conditions are discussed in more detail.

b) Uncapped anneals under conditions that favor reaction (1)

Many of the candidate gate oxides have high oxygen diffusivities. For example, the bulk diffusion length ($\sim\sqrt{D_v t}$) of oxygen in monoclinic, nanocrystalline zirconia is much greater than the gate dielectric thickness at typical annealing times [23]. Grain boundary diffusion coefficients in nanocrystalline zirconia are orders of magnitude larger than bulk coefficients [23]. Oxides with low oxygen permeability are thus highly prized gate oxides for MOSFET. Interfacial SiO_2 formation can also be avoided if high-*k* oxides are capped with a material with low oxygen permeability before the high-temperature anneal [11].

There is some discussion in the literature whether the interfacial layer formed between ZrO_2 or HfO_2 and Si under oxidizing conditions is SiO_2 or a silicate. Both types of interfacial layers have been reported [10,15,24-27]. The interface between interfacial SiO_2 and the high-*k* layer tends to be rough, and intermixing can be difficult to distinguish from roughness [28]. Any interface between interfacial SiO_2 and the overlaying HfO_2 or ZrO_2 layer requires Si-O-M (M =

Hf, Zr) “silicate” bonding that may be detected by some methods, such as x-ray photoelectron spectroscopy. Furthermore, because these layers are thin, this interfacial bonding will be a significant portion of the analyzed material. An interfacial SiO_2 layer is consistent with a mechanism that involves oxygen diffusion through the high-*k* layer and oxidation of silicon. **Amorphous** layers of MO_x and SiO_2 may subsequently interdiffuse, up to concentrations reaching the boundaries of the metastable extensions of the spinodal in the metal oxide-SiO_2 phase diagram [29]. A liquid miscibility gap exists in most metal oxide-SiO_2 pseudo-binary phase diagrams relevant for current high-*k* materials [29-31]. With respect to the interdiffusion of a **crystalline** ZrO_2 or HfO_2 layer and amorphous SiO_2, it has been shown that during zircon ($ZrSiO_4$) formation, Si^{4+} ions are the fastest diffusing species, whereas no Zr diffuses into amorphous SiO_2 [32]. Very little data exists on the diffusivity of ions in pure SiO_2, but it appears that the higher the positive charge of an ion, the lower is its diffusivity [33] and the diffusivities of Zr^{4+} and Hf^{4+} in SiO_2 are expected to be small. In summary, one may expect that interfacial SiO_2 layers contain little Zr or Hf. However, fine-grained and nonstoichiometric layers may show a different behavior [34], as will be discussed below.

c) Uncapped anneals under moderately reducing conditions

Next, possible reactions during uncapped anneals under conditions in which bare or SiO_2 covered Si would desorb SiO, as described by eqn. (2), are discussed. As shown in Fig. 2, at a given Si substrate temperature, the “etching” reactions (eqns. (2)) proceed at lower p_{O_2} than the SiO_2 reaction (eqn. (1)) [20,21]. These conditions are termed “moderately reducing” in this paper, and refer to p_{O_2}’s that favor SiO over SiO_2 formation for a bare or SiO_2 covered Si wafer but are not low enough to decompose the high-*k* oxide into its elemental constituents. In Fig. 2,

these p_{O_2}'s lie between the 'SiO-SiO_2" line and the stability lines of the high-*k* gate oxides (possible evaporation of high-*k* oxides at high temperatures is not considered here).

Some authors have suggested that SiO can desorb from Si surfaces that are capped with a high-*k* oxide [7,35]. Based on this assumption, SiO has been included in reactions that may explain interfacial silicide formation under conditions of low p_{O_2} (discussed in section III). The diffusion of SiO molecules through the high-*k* oxide is unlikely. Therefore, the "desorption" is more accurately described as Si going into solid solution in the high-*k* oxide, Si diffusion to the surface and recombination with adsorbed oxygen from the annealing atmosphere to form SiO gas. In case of a pre-existing SiO_2 layer at the interface, SiO_2 has to first decompose. These processes are shown schematically in Figs. 3(c-d).

It is important to consider the kinetic limitations for the processes shown in Figs. 3(c-d). At a given temperature and p_{O_2}, the desorption of SiO from the surface of a high-*k* stack likely depends on the gate dielectric thickness and the specific gate material [36]. Without direct evidence of SiO gas formation, observations of thinning of a pre-existing SiO_2 layer underneath a high-*k* oxide during annealing under moderately reducing conditions may also be due by decomposition and subsequent filling of O vacancies in the high-*k* dielectric as shown in Fig. 3(b) [8]. This mechanism is possible if the as-deposited high-*k* oxide was oxygen deficient, or if reducing processing atmospheres caused the high-*k* oxide to loose oxygen, because most high-*k* oxides under consideration have more negative free energies of formation than SiO_2. The nonstoichiometric high-*k* dielectric can reduce the interfacial SiO_2 in order to lower its free energy. Note that this reaction mechanism is nearly independent of the gate oxide thickness, as no long-range diffusion of Si is required and is also possible in presence of a capping layer. The

driving force for this thinning, based entirely on solid-state reactions, is the reduction of the free energy of the gate oxide, and not the free energy of formation of gaseous SiO.

Recently, SAYAN *et al.* [7] proposed an additional pathway, shown in Figs. 3(e-f), that involves direct evaporation of SiO from a Si surface exposed by pinholes. However, no direct experimental evidence of a correlation between the pinholes formation and reducing conditions exists, although pinholes have been reported in high-*k* oxides [28]. In particular, cross-section transmission electron microscopy should be employed to show that zones denuded of interfacial SiO_x exist around pinholes in stacks annealed under reducing conditions **before** the onset of silicide reaction. If silicide reaction occurs, lateral nonuniformities in the forming silicide (see Fig. 5) may break up the oxide layer.

The conditions for interfacial SiO_2 growth underneath a high-*k* stack were investigated by MARIA *et al* [5]. ZrO_2 thin films were annealed at 1000 ˚C under p_{O_2}'s between ~ 10^{-4} torr to 10^{-7} torr, controlled by adjusting the pressure of N_2 gas that contained about 1 ppm O_2. Figure 4 shows high-resolution transmission electron microscopy (HRTEM) images of the as-deposited and annealed ZrO_2/Si stacks [10]. After annealing at a p_{O_2} of about 10^{-4} torr, the thickness of the gate oxide stack increased [Fig. 4(b)] due to growth of the interfacial SiO_2-like layer. The ZrO_2 film annealed at a p_{O_2} in the range of 10^{-5} torr showed only a thin (~1 nm) interfacial SiO_2 layer [Fig 4(c)], i.e. neither extensive growth nor etching was observed. Lowering the p_{O_2} further, to about 10^{-7} torr, caused $ZrSi_2$ to form along the interface (Fig. 5). All samples were annealed under conditions for which reaction (2) dominates for bare silicon. Therefore, interfacial oxide growth of the ZrO_2 sample annealed ~10^{-4} torr may be due to a somewhat higher p_{O_2} during the experiment. However, it is likely that the kinetic limitations discussed above, i.e. the relative

rates of Si (and oxygen) escape through the overlying ZrO_2 layer versus the rate of SiO_2 formation, explain this result.

III. Silicide Formation

Many experiments have established that silicides in high-*k* stacks incorporating ZrO_2 or HfO_2 form under conditions of low p_{O_2}, such as in the experiment shown in Fig. 5, or during vacuum anneals [4,10]. Silicides have also been observed at the interface with the polycrystalline Si ("poly-Si") gate electrode [9,37,38]. Poly-Si gate electrode deposition using silane gas (SiH_4) causes very reducing atmospheres, i.e. very low p_{O_2}'s that may reduce high-*k* oxides such as ZrO_2. Recent studies have demonstrated that the silicide reaction between ZrO_2 films and poly-Si electrodes can be avoided by using less reducing conditions during the gate electrode deposition [8,38]. Although the relationship between low p_{O_2} and the tendency for ZrO_2 or HfO_2 to react with Si to a silicide is experimentally well established, the reaction pathways are less well understood.

Using bulk thermodynamic data from ref. [19], SCHLOM and co-workers predicted that stoichiometric ZrO_2 and HfO_2 are stable in contact with Si at typical annealing temperatures [1,2], i.e. that no silicide should form. Recently reported values of $\Delta H^{\circ}_{f,298\,\mathrm{K}}$ for Zr-silicides [39], which differ somewhat from the values in ref. [19] have been used to re-evaluate the thermodynamic stability of ZrO_2 in contact with Si [9]. In particular, the reactions

$$3\,\mathrm{Si} + 2\mathrm{ZrO_2} \longrightarrow \mathrm{ZrSi_2} + \mathrm{ZrSiO_4} \qquad (3)$$

$$2\,\mathrm{Si} + \mathrm{ZrO_2} \rightarrow \mathrm{ZrSi} + \mathrm{SiO_2} \qquad (4)$$

$$2\mathrm{Si} + 2\,\mathrm{ZrO_2} \rightarrow \mathrm{ZrSi} + \mathrm{ZrSiO_4} \qquad (5)$$

were reported to have a slightly negative values $\Delta G^{\circ}_{(3,4,5)}$ at 1000 K [9], implying that ZrO_2 is not stable in contact with Si at this temperature.

Only the $\Delta H^{\circ}_{f,298\,\mathrm{K}}$ values for ZrSi and $ZrSi_2$ were reported in ref. [39]. The heat capacities and entropies from ref. [19] were used to calculate the Gibbs free energies of the silicides (Table I). $\Delta G^{\circ}_{(3)}$ is about –3.2 kJ/mol at 1000 K. This is within the approximate uncertainty of the thermodynamic data, making the result of this calculation inconclusive. $\Delta G^{\circ}_{(4)}$ and $\Delta G^{\circ}_{(5)}$ are more negative (–11.02 kJ/mol and –17.5 kJ/mol, respectively) but are complicated and require partitioning of the reaction phase, leading to kinetic constraints, particularly when considering the short anneals in device fabrication. For example, the crystalline silicates are not observed under typical annealing conditions. More importantly, reactions (3-5) cannot explain the experimentally established relationship between low p_{O_2} and silicide reaction. However, the analysis in ref. [9] emphasizes the need for more reliable thermodynamic data for the candidate gate oxides and the metal silicides.

Including oxygen, which easily diffuses through most gate dielectrics, in the stability analysis, cannot predict silicide formation under typical annealing conditions. For example, for ZrO_2 to react with Si to form $ZrSi_2$ and O_2, the equilibrium p_{O_2} for the following reaction must be determined

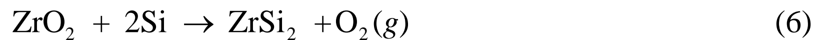

$$\mathrm{ZrO_2} + 2\mathrm{Si} \rightarrow \mathrm{ZrSi_2} + \mathrm{O_2}(g) \qquad (6)$$

At 1300 K, $\Delta G^{0}_{(6)}$ for reaction (6) is large and positive ($\Delta G^{0}_{(6)}$= 682 kJ/mol, using the free energy values in ref. [19] and Table I [19,39]). An equilibrium partial pressure p_{O_2} of 3.91×10^{-28} atm or 2.97×10^{-25} torr can be calculated from the equilibrium constant K_{eq}

($\Delta G^{o}_{(6)} = -RT\ln K_{eq} \approx -RT\ln p_{O2}$). Such low p_{O_2} cannot be obtained by adjusting the p_{O_2} directly and silicide formation according to reaction (6) should **not** occur for any viable p_{O_2} in high-*k* deposition processes. H_2/H_2O or CO/CO_2 mixtures are used to obtain such low p_{O_2}. It should be noted, however, that poly-Si gate electrode deposition using a silane or related process causes very low p_{O_2}'s due to the hydrogen gas involved. However, interfacial silicides have been observed at p_{O_2}'s much greater than 2.99×10^{-25} torr. For example, the $ZrSi_2$ shown in Fig. 5 formed after annealing at a p_{O_2} in the order of ~ 10^{-7} torr.

To explain why ZrO_2 (and HfO_2) react with Si at p_{O_2}'s much greater than the equilibrium p_{O_2} of reaction (6), two main reactions schemes have been proposed in literature [4-7,9,17,18,24]. The first approach is to include gaseous species, in particular SiO, as part of the thermodynamic analysis of interfacial reactions under reducing conditions [4-7,17,18]. A different explanation is based on nonstoichiometry of the high-*k* oxide [8]. Both schemes are evaluated in the following sections.

a) Reactions involving SiO

Several authors have proposed that SiO formation and/or consumption must be considered in the formation of interfacial silicides under moderately reducing conditions [4-7,17,18]. An important pre-requisite in these schemes is that no kinetic limitation exists for Si to escape to the surface of the high-*k* oxide and react with either adsorbed oxygen or oxygen from the gate oxide to form SiO. As discussed above, there is to date no conclusive experimental evidence that this indeed the case.

One may, however, evaluate these reactions solely with the goal to consider whether they are thermodynamically possible under typical annealing conditions in a hypothetical situation where no kinetic limitations exist for reactions (2). This analysis is carried out next. It will be shown that these schemes require additional kinetic boundary conditions should they lead to silicide formation.

For simplicity, it is assumed that no SiO_2 exists at the interface. For example, any SiO_2 may have already been reduced or desorbed via the reactions shown in Figs. 2 (b) or (c). The system under consideration then consists of the components ZrO_2, $ZrSi_2$, SiO (*g*), O_2 (*g*) and Si, as depicted in Fig. 6 (a). Furthermore, an infinite supply of Si is assumed.

Next, the maximum pressure tolerated by this system, if ZrO_2 is to react to form $ZrSi_2$, can be determined. In addition to eqns. (2a) and (3), the following reaction **may** occur:

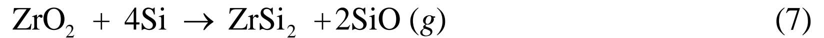

$$\mathrm{ZrO_2} + 4\mathrm{Si} \rightarrow \mathrm{ZrSi_2} + 2\mathrm{SiO}\,(g) \qquad (7)$$

At 1300 K, $\Delta G^0_{(7)}$ for reaction (7) is positive ($\Delta G^0_{(7)}$= 259 kJ/mol), yielding an equilibrium SiO partial pressure p_{SiO} of 6.35×10^{-6} atm or 4.82×10^{-3} torr, as calculated from the equilibrium constant ($\Delta G^o_{(7)} = -RT\ln K_{eq} \approx -RT\ln p^2_{SiO}$). Therefore, for SiO partial pressures of less than 4.82×10^{-3} torr, reaction (7) **may** occur.

At 1300 K, $\Delta G^0_{(2a)}$ for reaction (2a) is negative ($\Delta G^0_{(2a)}$= – 423 kJ/mol). With $\Delta G^o_{(2a)} = -RT\ln K_{eq} \approx -RT\ln p^2_{SiO} / p_{O2}$, this yields

$$\frac{p^2_{SiO}}{p_{O2}} = 1.03\times10^{17}\,\mathrm{atm}, \qquad (8)$$

consistent with the partial pressures obtained from reactions (6) and (7), i.e., $\left(6.35\times10^{-5}\,\mathrm{atm}\right)^2 / 3.91\times10^{-28}\,\mathrm{atm} = 1.03\times10^{17}\,\mathrm{atm}$.

Therefore, for ZrO_2, Si, and $ZrSi_2$ to be in equilibrium at 1300 K with a gaseous atmosphere of SiO and O_2, the atmosphere must be of composition $p_{SiO} = 6.35\times10^{-6}$ atm and $p_{O_2} = 3.91\times10^{-28}$ atm. If $p_{O_2} + p_{SiO}$ is less than ~ 6.35×10^{-6} atm, the silicide reaction is favorable.

In real annealing experiments, the p_{O_2} is greater than ~ 4×10^{-28} atm. In this case, reaction (2a) will be shifted to the right, i.e. Si will be etched and the SiO partial pressure increases, shifting both reaction (6) and (7) to the left, i.e. no silicide will be formed. Therefore, silicide formation according to reaction (7) is only favorable if SiO formed by reactions (2a) and (7) is continuously **removed** from the system and the p_{SiO} is locally reduced below 6.35×10^{-6}atm or 4.82×10^{-3} torr.

Some authors have suggested recycling of SiO via continuous SiO_2 formation and etching by reactions of ZrO_2 with SiO to explain the formation of silicide [4,18]. Given the typical annealing conditions of either flowing N_2 gas or pumping, such a SiO "recycling" reaction is unlikely.

In summary, these reactions can result in silicide formation only under **kinetic** boundary conditions that should be verified by additional experimental studies. In particular, *(i)* sufficient Si diffusion through the high-*k* oxide, and *(ii)* removal of SiO from the system are conditions should reaction (7) be involved in silicide reactions. Reaction (7) also cannot explain why silicide reactions are observed in capped stacks, i.e., after deposition of the polysilicon gate electrode when SiO gas cannot form. In the next section, a recently proposed alternative mechanism of silicide formation is discussed.

b) High-*k* Oxygen Deficiency

High-*k* oxides are stable down to very low p_{O_2} (see the stability lines in Fig. 2). However, high-*k* films deposited by physical vapor deposition techniques or metal oxidation may be oxygen deficient, particularly under growth conditions that avoid extensive interfacial SiO_2 formation [40]. Reducing atmospheres during processing may cause oxygen deficiency. Recently, a mechanism for the silicide formation involving oxygen deficiency has been proposed [8]. The free energy of the oxygen deficient film/substrate system can be lowered by oxidation, if oxygen is available, or by reaction of excess metal with Si, leaving behind a stoichiometric oxide:

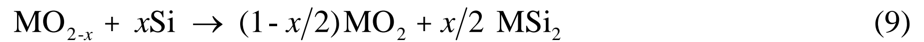

$$\mathrm{MO}_{2\text{-}x} + x\mathrm{Si} \rightarrow (1 - x/2)\mathrm{MO}_2 + x/2\ \mathrm{MSi}_2 \qquad (9)$$

The difference in the free energy between the stoichiometric and the nonstoichiometric high-*k* oxide acts as an additional driving force for the silicide reaction. PERKINS *et al.* [8] expressed reaction (9) by employing the defect reaction (using ZrO_2 as example):

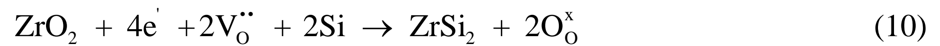

$$\mathrm{ZrO}_2 + 4e' + 2V_O^{\bullet\bullet} + 2\mathrm{Si} \rightarrow \mathrm{ZrSi}_2 + 2O_O^x \qquad (10)$$

PERKINS *et al.* determined that the reaction enthalpy for eqn. (10), i.e., the driving force for the silicide reaction, is negative [8]. The reaction steps behind eqn. (10) [8] are the decomposition of part of the nonstoichiometric ZrO_2

$$\mathrm{ZrO}_2 \rightarrow \mathrm{Zr} + \mathrm{O}_2 \qquad (10a)$$

the reaction of Zr with Si to form $ZrSi_2$

$$\mathrm{Zr} + 2\mathrm{Si} \rightarrow \mathrm{ZrSi}_2 \qquad (10b)$$

and the filling of two oxygen vacancies in the other part of the nonstoichiometric ZrO_2 by the oxygen of the decomposition reaction

$$O_2 + 2V_O^{\bullet\bullet} + 4e' \rightarrow 2O_O^x \tag{10c}$$

The processes are as shown schematically in Fig. 6 (b). Note that O_2 appears in reaction (10a) on the right side and in (10c) on the left side, thus does not appear in the summation (eqn. (10)), which is entirely a solid-state reaction and does not depend on the p_{O_2}. The experimentally observed p_{O_2} dependence of the silicide reaction in this mechanism arises from the oxygen deficiency of the high-*k* oxide created by reducing conditions during annealing or processing, which then promotes the silicide formation according to eqn. (10). It is thus necessary to determine the oxygen vacancy concentration for which the reaction (10) will proceed. The equilibrium constant (K_{red}) for the reduction reaction for ZrO_2

$$O_O^x \rightarrow V_O^{\bullet\bullet} + 2e' + 1/2\, O_2(g), \tag{11}$$

is given by

$$K_{red} = \left[V_O^{\bullet\bullet}\right]\left[e'\right]^2 p_{O2}^{1/2} \tag{12}$$

Here the relative concentration of oxygen ions on their sites, $\left[O_O^x\right]$, has been left out of the denominator since it is approximately unity if the concentration of oxygen vacancies is dilute. With the charge neutrality condition

$$2\left[V_O^{\bullet\bullet}\right] = \left[e'\right] \tag{13}$$

K_{red} becomes

$$K_{red} = 4\left[V_O^{\bullet\bullet}\right]^3 p_{O2}^{1/2} \tag{14}$$

The free energy change for the reduction reaction (11) is given by

$$\Delta G_{red} = -RT \ln K_{red} \tag{15}$$

With ΔG_{red}, and the free energies of reactants and products of eqn. (10), the free energy change for reaction (10) at a given temperature can be calculated. The oxygen vacancy concentration for which the silicide reaction (10) will become thermodynamically favorable may then be determined (using the charge neutrality condition (13)):

$$\Delta G^{o}_{(10)} = -RT \ln K_{eq} = -RT \ln\left(1 \Big/ \left(16 \cdot \left[V_O^{\bullet\bullet} \right]^6 \right) \right) \tag{16}$$

To estimate the oxygen vacancy concentration for ZrO_2 or HfO_2, for which reaction (10) would proceed to the right, K_{red} for the reduction reaction has to be known, in addition to the free energies the oxides and silicides. Some data is available for bulk ZrO_2, but only limited data exists for HfO_2. In the following, we estimate the equilibrium oxygen vacancy concentration for **bulk** oxides at 1300 K, using data from XUE [41], WANG *et al.* [42] and TALLAN *et al*. [43]. Bulk thermodynamic data may be suited to understand trends but are likely of very limited value for these nanocrystalline, ultrathin films, as shown in recent investigations of nanocrystalline ceria films [44,45].

The equilibrium constant for the reduction reaction as a function of temperature for **monoclinic** zirconia was determined by XUE [41], as described in detail in the appendix of this paper. Using XUE's data, K_{red} has a value of 1.27×10^{-17} at 1300 K. Using eqn. (15), ΔG°_{red} for the reduction reaction (10) is ~ 420 kJ/mol. The free energy change for reaction (10), $\Delta G^{o}_{(10)}$, is – 158 kJ/mol at 1300 K, calculated from $\Delta G^{o}_{(10a)} + \Delta G^{o}_{(10b)} + \Delta G^{o}_{(10c)}$. Using eqn. (16), the equilibrium concentration of oxygen vacancies is ~ 6 %. Therefore, for any monoclinic ZrO_{2-x} film with oxygen nonstoichiometry x greater than ~ 0.06, the silicide may form at 1300 K.

In thin ZrO_2 films, the tetragonal polymorph, rather than the low-temperature equilibrium monoclinic phase, is often observed [46,47]. Possible reasons include high concentrations of oxygen vacancies or the small grain size of the films, because for the monoclinic phase to be

stable, the grain size has to be greater than a critical value [48]. This critical grain size is smaller for HfO_2 than for ZrO_2 [48,49]. As shown in the appendix, the equilibrium constant for reaction (11) for tetragonal ZrO_2 may be obtained from WANG and OLANDER [42]. Extrapolating the equilibrium constant for tetragonal ZrO_2 to 1300 K, the oxygen vacancy equilibrium concentration would be about 0.02%. Based on the available thermodynamic data, tetragonal ZrO_2 has to be less oxygen deficient than monoclinic ZrO_2 to react with Si to form the silicide. Although they are expected to be different, the large discrepancy between the results for monoclinic and tetragonal ZrO_2 likely also illustrates the great uncertainty in the available thermodynamic data. HfO_2 films are reported to be more resistant to silicide formation than ZrO_2 [50,51]. Only one study in the literature by TALLAN *et al.* reports weight change data that can be used to interpret the point defect chemistry of HfO_2 [43]. However, the nonstoichiometry in this study was very small and there is great uncertainty in the data, as shown in the appendix.

An important issue that arises with the proposed reaction mechanism and that should be addressed in further experimental studies are the very low p_{O_2}'s that are predicted by reaction (14) that would be necessary for an **initially stoichiometric** high-*k* oxide to become oxygen deficient enough for the silicide reaction (10) to become favorable. This statement even holds if more accurate vacancy formation energies would be used in the equations. Although lower vacancy formation energies (as reported for nanocrystalline materials) increase the oxygen deficiency at a given p_{O_2}, they lower at the same time the driving force for reaction (10), thus requiring larger defect concentrations for the silicide reaction. A possible reason why the proposed reaction mechanism is nevertheless a likely explanation for silicide formation is that thin films are more nonstoichiometric, due to impurities, and the proximity of interfaces and surfaces. Even more importantly, thin films are likely not in thermodynamic equilibrium.

In summary, despite their limited quantitative value, the estimates show that very small oxygen deficiency may promote silicide reaction in ZrO_2 or HfO_2 thin films. Experimental detection of such small nonstoichiometries in ultrathin films is challenging.

IV. Silicate Formation

Several experimental studies have shown extensive silicate formation at the interface between rare earth and related oxide films (such as Y_2O_3, Gd_2O_3 and La_2O_3) and Si [11,13,14,52]. These reactions are likely due to excess oxygen, such as OH or related species that are incorporated in the film, or O_2 in the annealing atmosphere. Stoichiometric films show no interfacial silicate layers, and epitaxial growth of rare oxide films on silicon is possible [53-56]. Interfacial rare earth silicates may also form by consuming interfacial SiO_2 layers. For example, annealing of La_2O_3 in oxygen containing atmospheres results in competing reactions of interfacial SiO_2 formation by oxygen diffusion through the high-*k* film, Si oxidation, and reaction of this SiO_2 to La silicate [57]. In contrast to HfO_2 or ZrO_2, rare earth and related oxides readily form silicates. For example, at 1300 K, the free energy changes for the silicate reactions from the oxides

$$SiO_2 + ZrO_2 \rightarrow ZrSiO_4 \quad (17)$$

$$SiO_2 + Y_2O_3 \rightarrow Y_2SiO_5 \quad (18)$$

are $\Delta G^{\circ}_{(17)}$= -2.96 kJ/mol [19], and $\Delta G^{\circ}_{(18)}$= - 135 kJ/mol [19,58], respectively. Thus there is a much greater driving force to form the Y-silicate than the Zr-silicate, if, for example, SiO_2 is present at the interface between Si and the high-*k* oxide.

Furthermore, rare earth and related oxides strongly absorb and react with water [59,60]. Hydroxyl ions may also be present in low temperature chemical vapor deposited films. In the

extreme case of a film that has completely reacted to a hydroxide, the following reaction may take place during annealing:

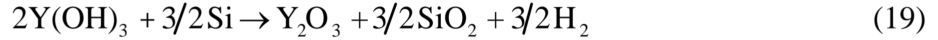

$$2Y(OH)_3 + 3/2\,Si \rightarrow Y_2O_3 + 3/2\,SiO_2 + 3/2\,H_2 \quad (19)$$

Recent thermodynamic data shows that the binary oxides, Y_2O_3 and SiO_2, are unstable with respect to the reaction to form Y-silicates (eqn. 18). The reaction products of eqn. (19) will form the silicate:

$$Y_2O_3 + SiO_2 \rightarrow Y_2SiO_5 \quad (20)$$

The silicate reaction may proceed further:

$$Y_2SiO_5 + SiO_2 \rightarrow Y_2Si_2O_7 \quad (21)$$

Recent results show that *in situ* capping layers can successfully prevent extensive SiO_2 formation at the interface with silicon [11,14]. However, excess oxygen incorporated into the films during chemical vapor deposition causes silicate formation, even it is not sufficient for extensive Si-oxidation [11]. Interfacial SiO_2 in uncapped or *ex situ* capped CVD samples [52] probably forms once the silicate reaction is completed and enough excess oxygen is available, or if silicate formation is kinetically limited, for example by the rate of Si diffusion from the substrate.

It is interesting to note that the silicate reaction layers are always amorphous, even if the rare-earth oxide film had crystallized before the reaction [11,52]. Amorphization has been observed in the reaction of metal bilayers [61] as well as TiO_2/ZrO_2 diffusion couples [62]. It is believed that the formation of amorphous interlayers is related to significant mobility differences [63]. In this case, if Si diffuses more easily in Y_2O_3 than Y in SiO_2 (or Si), then the Y_2O_3 layer

becomes supersaturated with Si, and crystalline Y-silicate should nucleate. However, if the nucleation barrier is high, it will form an amorphous silicate, in particular if this leads to a large change in free energy.

V. Conclusions

Si compatibility is just one of many requirements for alternative gate dielectrics for Si-based MOSFETs, but nevertheless proves to be a challenging task. Binary oxides that are stable or potentially stable in contact with Si can show interface reactions due to high-*k* nonstoichiometry and high oxygen diffusivities. Thermodynamic analysis of the relevant reactions may indicate ways to improve the stability of high-*k* interfaces. In particular,

- capping layers that prevent oxygen diffusion through the high-*k* material,
- less reducing conditions during processing, and
- control of thin film stoichiometry

may potentially alleviate most of the thermal stability problems, including for ZrO_2 [8]. Oxygen excess in the films must carefully be avoided to prevent extensive silicate layers in case of rare-earth oxides, or SiO_2 in case of ZrO_2 or HfO_2. Oxygen deficiency must be avoided to prevent silicide reactions.

An even more challenging task may be to avoid the formation of interfacial SiO_2 during high-*k* deposition. While reducing conditions (below the SiO/SiO_2 line in Fig. 2) should result in SiO_2-free interfaces, the high-*k* oxide may become oxygen deficient at low p_{O_2}'s, resulting in poor electrical properties and stability problems (silicide formation). For example, shown in Fig. 2 are calculated p_{O_2}'s and temperatures at which **bulk monoclinic** ZrO_{2-x} would show an

(arbitrarily chosen) oxygen deficiency of $x = 0.002$. The temperature- p_{O_2} field between these data points and the SiO-SiO_2 line represents a processing window within which SiO_2 formation is avoided and the oxygen deficiency remains smaller than 0.002. The smaller the required oxygen deficiency, the narrower the processing window becomes. The values were calculated using XUE's data [41] for bulk ZrO_2. Recent research has shown that thin, nanocrystalline films show much lower oxygen vacancy formation enthalpies. For example, nanocrystalline ceria shows an activation enthalpy for oxygen vacancies of ~ 1eV whereas that of a single crystal is ~ 2 eV [45]. Lower activation enthalpy for oxygen vacancies may narrow or even eliminate the processing window. Thus, achieving alternative gate dielectric stacks with low EOT becomes challenging due to the need to sufficiently oxidize the high-*k* material without oxidizing the underlying Si. Oxygen diffusivities, oxygen (and metal) point defect formation energies and the hygroscopic nature of the oxide should become important selection criteria for future alternative gate dielectric materials.

Acknowledgements

The author would like to thank Prof. Darrell Schlom of Penn State, Profs. Carlos Levi and Jim Speck of UCSB for many useful discussions, Dr. Wei-E Wang of Intel Corp. for alerting her to ref. [43] and Ms. Yan Yang for help with extracting the data from ref. [43]. The experimental results shown in Figs. 4 and 5 were obtained in collaboration with Profs. Jon-Paul Maria and Angus Kingon of NCSU. The research was supported by Sematech and SRC through the FEP Center.

Appendix

A1. Review of literature data on the nonstoichiometry and equilibrium constants for ZrO_2

Using XUE's notation, the absolute deviation from stoichiometry, δ, in the formula $MO_{2+\delta}$ (M = Hf or Zr) can be expressed as

$$\delta = \Delta\delta + \delta^{\circ} \tag{A.1}$$

where δ° is the deviation of stoichiometry at the reference point and $\Delta\delta$ is calculated from measured mass changes Δm, using the equation given by XUE [41]:

$$\Delta\delta \approx \left[\frac{2 \cdot M_O + M_M}{M_O}\right] \cdot \frac{\Delta m}{m^{\circ}} \tag{A.2}$$

where M_M and M_O denote the atomic weights of the metal (Hf or Zr) and O, respectively, and m° is the sample mass. δ° can be obtained by fitting the weight change data with appropriate point defect models [41]. For ZrO_2, XUE assumed a defect model with completely ionized Zr vacancies at high p_{O_2}'s, and completely ionized oxygen vacancies at low p_{O_2}'s. The relation between δ and the oxygen partial pressure is then given by

$$\delta = A \cdot p_{O2}^{1/5} - B \cdot p_{O2}^{-1/6} = \Delta\delta + \delta^{\circ} \tag{A.3}$$

A and B are positive constants [41]. The 1/5 exponent reflects a defect model with metal vacancies, the –1/6 exponent oxygen vacancies. For example, rearranging eq. (14) yields

$$\left[V_O^{\bullet\bullet}\right] = K_{red}^{1/3} \cdot 4^{-1/3} \cdot p_{O2}^{-1/6} = K_{11} \cdot p_{O2}^{-1/6} \tag{A.4}$$

Here, the equilibrium constant K_{11} was introduced to replace K_{red} to be consistent with XUE's notation, which is K_{11} for our reaction (11), i.e.,

$$K_{11} = \left(\frac{K_{red}}{4}\right)^{1/3} = \left[V_O^{\bullet\bullet}\right] p_{O2}^{1/6} \quad \text{(A.5)}$$

K_{11} can also be expressed as

$$K_{11} = A_{11} \exp\left(-\frac{\Delta H_{11}}{kT}\right) \quad \text{(A.6)}$$

Fitting of the experimental data ($\Delta\delta$) is used to determine A, B (K_{11}) and δ° [41]. At 1300 K, K_{11} for monoclinic ZrO_2 has a value of 1.47×10^{-6} (cf. Fig. 4 in XUE's paper). K_{11} was used to calculate K_{red} to perform the calculations for the silicide reactions in the main body of this paper. XUE found great uncertainty in the K_{11} value derived from their experimental data for tetragonal ZrO_2, due to the small nonstoichiometry.

WANG *et al.* determined K_{11} for **tetragonal** ZrO_2 (stable above 1478 K) [42]:

$$\ln K_{11} = 0.43 - \frac{22700}{T} \quad \text{(A.7)}$$

A2. Literature data on nonstoichiometry of HfO_2

TALLAN *et al.* [43] measured the weight changes of HfO_2 as a function of p_{O_2} to determine its defect chemistry. TALLAN *et al.* interpreted the weight change as proportional to $p_{O2}^{1/5}$, which corresponds to a defect model with fully ionized Hf vacancies as the dominant point defects [43]. To be consistent with XUE's analysis, values of $\Delta\delta$ were calculated using the mass changes Δm reported by TALLAN *et al*. [43] and eqn. (A.2) and are shown in Fig. A.1.

Fitting the data to eqn. (A.3) yielded inconclusive results because the deviation from stoichiometry at the p_{O_2}'s in TALLAN *et al.*'s experiments was so small that only for two temperatures, 1000 ˚C and 1500 ˚C, the data fits resulted in positive values for constant *B*. With K_{11} obtained at 1000 ˚C (5.897×10^{-8}) and the Gibbs free energy data for $HfSi_2$ given in Table I

[64], the equilibrium concentration of oxygen vacancies for eqn. (10) at this temperature is about 0.6%.

TALLAN *et al.* used their data to determine the activation energy of the reaction for completely ionized Hf vacancies [43]. Using XUE's notation

$$1/2\,\mathrm{O_2}(g) \rightarrow \mathrm{V_{Hf}^{''''}} + 4h^{\bullet} + \mathrm{O_O^x} \qquad \text{(A.8)}$$

$$K_{13} = \frac{\left[V_{Hf}^{''''}\right]}{p_{O2}^{1/5}} = A_{13} \cdot \exp\left(-\frac{\Delta H_{13}}{kT}\right) \qquad \text{(A.9)}$$

TALLAN *et al.*'s data were fit to eqn. (A.3) for 1000 ˚C and 1500 ˚C, whereas for the intermediate temperatures a fit omitting the second term in eqn. (A.3) was used to obtain K_{13}. The results and a comparison with XUE's data for ZrO_2 are shown in Table A.I. However, the data could be fit equally well if an oxygen interstitial model was used instead of Hf vacancies, i.e. using an exponent of 1/6 instead of 1/5 in eqn. (A.3).

References

[1] K. J. Hubbard and D. G. Schlom, J. Mater. Res. **11,** 2757-2776 (1996).

[2] D. G. Schlom, C. A. Billmann, J. H. Haeni, J. Lettieri, P. H. Tan, R. R. M. Held, S. Völk, and K. J. Hubbard, Appl. Phys. A (to be published) (2003).

[3] Y.-M. Sun, J. Lozano, H. Ho, H. J. Park, S. Veldman, and J. M. White, Appl. Surf. Sci. **161,** 115-122 (2000).

[4] T. S. Jeon, J. M. White, and D. L. Kwong, Appl. Phys. Lett. **78,** 368-370 (2001).

[5] J. P. Maria, D. Wicaksana, A. I. Kingon, B. Busch, H. Schulte, E. Garfunkel, and T. Gustafsson, J. Appl. Phys. **90,** 3476-3482 (2001).

[6] M. A. Gribelyuk, A. Callegari, E. P. Gusev, M. Copel, and D. A. Buchanan, J. Appl. Phys. **92,** 1232-1237 (2002).

[7] S. Sayan, E. Garfunkel, T. Nishimura, W. H. Schulte, T. Gustafsson, and G. D. Wilk, J. Appl. Phys. **94,** 928-934 (2003).

[8] C. M. Perkins, B. B. Triplett, P. C. McIntyre, K. C. Saraswat, and E. Shero, Appl. Phys. Lett. **81,** 1417-1419 (2002).

[9] M. Gutowski, J. E. Jaffe, C.-L. Liu, M. Stoker, R. I. Hedge, R. S. Rai, and P. J. Tobin, Appl. Phys. Lett. **80,** 1897-1899 (2002).

[10] S. Stemmer, Z. Chen, R. Keding, J.-P. Maria, D. Wicaksana, and A. I. Kingon, J. Appl. Phys. **92,** 82-86 (2002).

[11] S. Stemmer, D. O. Klenov, Z. Q. Chen, D. Niu, R. W. Ashcraft, and G. N. Parsons, Appl. Phys. Lett. **81,** 712-714 (2002).

[12] M. Copel, E. Cartier, V. Narayanan, M. C. Reuter, S. Guha, and N. Bojarczuk, Appl. Phys. Lett. **81,** 4227-4229 (2002).

[13] G. A. Botton, J. A. Gupta, D. Landheer, J. P. McCaffrey, G. I. Sproule, and M. J. Graham, J. Appl. Phys. **91,** 2921-2928 (2002).

[14] B. W. Busch, J. Kwo, M. Hong, J. P. Mannaerts, B. J. Sapjeta, W. H. Schulte, E. Garfunkel, and T. Gustafsson, Applied Physics Letters **79,** 2447-2449 (2001).

[15] M. Copel, M. Gribelyuk, and E. Gusev, Appl. Phys. Lett. **76,** 436-438 (2000).

[16] B. W. Busch, W. H. Schulte, E. Garfunkel, T. Gustafsson, W. Qi, R. Nieh, and J. Lee, Phys. Rev. B **62,** R13290-R13293 (2000).

[17] J. P. Chang and Y.-S. Lin, Appl. Phys. Lett. **79,** 3824-3826 (2001).

[18] K. Muraoka, Appl. Phys. Lett. **80,** 4516-4518 (2002).

[19] I. Barin, *Thermochemical Data of Pure Substances*, Vol. I and II, 3rd ed. (VCH, Weinheim, 1995).

[20] J. J. Lander and J. Morrison, J. Appl. Phys. **33,** 2089-2092 (1962).

[21] F. W. Smith and G. Ghidini, J. Electrochem. Soc. **129,** 1300-1306 (1982).

[22] D. Starodub, E. P. Gusev, E. Garfunkel, and T. Gustafsson, Surf. Rev. Lett. **6,** 45-52 (1999).

[23] U. Brossmann, R. Würschum, U. Södervall, and H.-E. Schneider, J. Appl. Phys. **85,** 7646-7654 (1999).

[24] C. M. Perkins, B. B. Triplett, P. C. McIntyre, K. C. Saraswat, S. Haukka, and M. Tuominen, Appl. Phys. Lett. **78,** 2357-2359 (2001).

[25] T. Yamaguchi, H. Satake, N. Fukushima, and A. Toriumi, Appl. Phys. Lett. **80,** 1987-1989 (2002).

[26] Y.-S. Lin, R. Puthenkovilakam, J. P. Chang, C. Bouldin, I. Levin, N. V. Nguyen, J. Ehrstein, Y. Sun, P. Pianetta, T. Conrad, W. Vandervorst, V. Venturo, and S. Selbrede, J. Appl. Phys. **93,** 5945-5952 (2003).

[27] O. Renault, D. Samour, J.-F. Damlencourt, D. Blin, F. Martin, S. Marthon, N. T. Barrett, and P. Besson, Appl. Phys. Lett. **81,** 3627-3629 (2002).

[28] P. S. Lysaght, B. Foran, G. Bersuker, P. J. Chen, R. W. Murto, and H. R. Huff, Appl. Phys. Lett. **82,** 1266-1268 (2003).

[29] S. Stemmer, Z. Chen, C. Levi, P. S. Lysaght, B. Foran, J. A. Gisby, and J. R. Taylor, Jap. J. Appl. Phys. **42,** 3593-3597 (2003).

[30] S. S. Kim, Y. Y. Park, and T. H. Sanders, J. Alloys Compounds **321,** 84-90 (2001).

[31] V. B. M. Hageman and H. A. J. Oonk, Phys. Chem. Glasses **27,** 194-198 (1986).

[32] C. Veytizou, J. F. Quinson, O. Valfort, and G. Thomas, Solid State Ionics **139,** 315-323 (2001).

[33] G. H. Frischat, *Ionic Diffusion in Oxide Glasses* (Trans Tech Publications, 1975).

[34] K. R. Coffey and K. Barmak, Acta metall. mater. **42,** 2905-2911 (1994).

[35] M. Copel, Appl. Phys. Lett. **82,** 1580-1582 (2003).

[36] E. Garfunkel, personal communication (2003).

[37] T. Z. Ma, S. A. Campbell, R. Smith, N. Hoilien, B. Y. He, W. L. Gladfelter, C. Hobbs, D. Buchanan, C. Taylor, M. Gribelyuk, M. Tiner, M. Coppel, and J. J. Lee, IEEE Trans. Electron Dev. **48,** 2348-2356 (2001).

[38] A. Callegari, E. Gousev, T. Zabel, D. Lacey, M. Gribelyuk, and P. Jamison, Appl. Phys. Lett. **81,** 4157-4158 (2002).

[39] S. V. Meschel and O. J. Kleppa, J. Alloys Compounds **274,** 193-200 (1998).

[40] J. Lettieri, J. H. Haeni, and D. G. Schlom, J. Vac. Sci. Technol. A **20,** 1332-1340 (2002).

[41] J. Xue, J. Electrochem. Soc. **138,** 36C-40C (1991).

[42] W.-E. Wang and D. R. Olander, J. Am. Ceram. Soc. **76,** 1242-1248 (1993).

[43] N. M. Tallan, W. C. Tripp, and R. W. Vest, J. Am. Ceram. Soc. **50,** 279-283 (1967).

[44] I. Kosaki, V. Petrovsky, and H. U. Anderson, J. Am. Ceram. Soc. **85,** 2646-2650 (2002).

[45] Y.-M. Chiang, E. B. Lavik, I. Kosacki, H. L. Tuller, and J. Y. Ying, J. Electroceram. **1,** 7-14 (1997).

[46] C. Zhao, G. Roebben, M. Heyns, and O. V. D. Biest, Key. Eng. Mat. **206-2,** 1285-1288 (2002).

[47] X. Wu, D. Landheer, M. J. Graham, H.-W. Chen, T.-Y. Huang, and T.-S. Chao, J. Cryst. Growth **250,** 479-485 (2003).

[48] R. C. Garvie, J. Phys. Chem. **69,** 1238 (1965).

[49] J. Wang, H. P. Li, and R. Setvens, J. Mater. Sci. **27,** 5397-5430 (1992).

[50] S. J. Lee, H. F. Luan, W. P. Bai, C. H. Lee, T. S. Jeon, Y. Senzaki, D. Roberts, and D. L. Kwong, Tech. Dig. Int. Electron Devices Meet. (2000).

[51] L. Kang, K. Onishi, Y. Jeon, B. H. Lee, C. Kang, W.-J. Qi, R. Nieh, S. Gopalan, R. Choi, and J. C. Lee, Tech. Dig. Int. Electron Devices Meet. (2000).

[52] D. Niu, R. W. Ashcraft, Z. Chen, S. Stemmer, and G. N. Parsons, Appl. Phys. Lett. **81,** 676-678 (2002).

[53] S. Guha, N. A. Bojarczuk, and V. Narayanan, Appl. Phys. Lett. **80,** 766-768 (2002).

[54] G. Apostolopoulos, G. Vellianitis, A. Dimoulas, M. Alexe, R. Scholz, M. Fanciulli, D. T. Dekadjevi, and C. Wiemer, Appl. Phys. Lett. **81,** 3549-3551 (2002).

[55] J. Kwo, M. Hong, A. R. Kortan, K. L. Queeney, Y. J. Chabal, R. L. Opila, D. A. Muller, S. N. G. Chu, B. J. Sapjeta, T. S. Lay, J. P. Mannaerts, T. Boone, H. W. Krautter, J. J. Krajewski, A. M. Sergnt, and J. M. Rosamilia, J. Appl. Phys. **89,** 3920-3927 (2001).

[56] J. P. Liu, P. Zaumseil, E. Bugiel, and H. J. Osten, Appl. Phys. Lett. **79,** 671-673 (2001).

[57] S. Stemmer, J. P. Maria, and A. I. Kingon, Appl. Phys. Lett. **79,** 102-104 (2001).

[58] O. Fabrichnaya, H. J. Seifert, R. Weiland, T. Ludwig, F. Aldinger, and A. Navrotsky, Z. Metallkd. **92,** 1083-1097 (2001).

[59] Y. Kuroda, H. Hamano, T. Mori, Y. Yoshikawa, and M. Nagao, Langmuir **16,** 6937-6947 (2000).

[60] D. Niu, R. W. Ashcraft, and G. N. Parsons, Appl. Phys. Lett. **80,** 3575-3577 (2002).

[61] K.-N. Tu, J. W. Mayer, and L. C. Feldman, *Electronic Thin Film Science for Electrical Engineers and Materials Scientists* (Macmillan, New York, 1992).

[62] H. Shin, M. Agarwal, M. R. D. Guire, and A. H. Heuer, J. Am. Ceram. Soc. **79,** 1975-1978 (1996).

[63] Y.-T. Cheng, W. L. Johnson, and M.-A. Nicolet, Appl. Phys. Lett. **47** (1985).

[64] J.-C. Zhao, B. P. Bewlay, M. R. Jackson, and Q. Chen, J. Phase Equil. **21,** 40-45 (2000).

Table I: Gibbs energies (as used by BARIN [19]) and free energies of formation from the elements in kJ/mol of the silicides at 1000 K and 1300 K. See text for explanation.

	G (1000 K)	G (1300 K)	ΔG_f (1000 K)	ΔG_f (1300 K)
ZrSi	-237	-275	-155	-153
Ref. [19]				
ZrSi	-271	-309	-189	-187
Ref. [19] +[39]				
$ZrSi_2$	-266	-317	-153	-149
Ref. [19]				
$ZrSi_2$	-288	-338	-173	-171
Ref. [19] +[39]				
$HfSi_2$	-296	-342	-178	-168
Ref. [64]				

Table A.I: Activation enthalpies for oxygen vacancy and Hf-vacancy formation determined in the literature for ZrO_2 and HfO_2.

Oxide	Activation enthalpy for oxygen vacancies (eqn. (A.6))	Activation enthalpy for Hf vacancies (eqn. (A.9))	References
Monoclinic ZrO_2	$\Delta H_{11} = 1.67$ eV	$\Delta H_{13} = 0.11$ eV	XUE [41]
Tetragonal ZrO_2	$\Delta H_{11} = 1.96$ eV	$\Delta H_{13} = 0.67$ eV	XUE [41], and WANG *et al*. [42]
Monoclinic HfO_2	Insufficient data available	$\Delta H_{13} = 0.24$ eV	TALLAN *et al.* [43]

Figure Captions

Figure 1

Schematic illustrating reported interface phases in high-*k* gate stacks: (a) SiO_{2-x} interface layer during deposition or after uncapped annealing in an O_2 containing atmosphere and sufficiently high partial pressures of O_2, (b) interfacial silicate layers frequently observed underneath rare-earth oxides, (c) interfacial silicide after uncapped anneals under reducing conditions, and (d) silicide at the interface with the poly-Si gate electrode.

Figure 2

Stability lines showing the equilibrium p_{O_2} for the reactions M + $O_2 \rightarrow MO_2$, where M = Hf, Zr and Si, respectively [19]. Above the stability line, the oxide is thermodynamically stable. Also shown are the experimentally determined conditions for growth of SiO_2 on Si (solid line) after ref. [21] and an extrapolation of the data (dashed line). Below the line, SiO desorbes, above the line, SiO_2 grows. Filled circles are p_{O_2}'s for which monoclinic, bulk ZrO_{2-x} would show a oxygen deficiency of $x = 0.002$, as calculated from Xue's data: Fig. 4 in ref. [41] and eqns. (A.5) and (A.6) ($A_{11} = 4.37$, $\Delta H_{11} = 1.67$ eV).

Figure 3

Schematic of possible high-*k* gate stack reactions during uncapped anneals if O_2 is present in the annealing atmosphere. Small black circles represent atomic oxygen, large black circles O_2 molecules, open circles Si, squares are oxygen vacancies and grey circles are SiO. (a) O_2 present

in the annealing or growth atmosphere dissociates to atomic oxygen and diffuses through the high-*k* oxide, followed by reaction to SiO_2 at the Si interface; (b-f): moderately reducing conditions; (b) interfacial SiO_2 decomposes and oxygen fills pre-existing oxygen vacancies in the high-*k* oxide, Si remains at the interface; (c) interfacial SiO_2 decomposes whereby both Si and oxygen diffuse through the high-*k* oxide and recombine to form SiO gas; (d) similar process as in (c), but assuming that no SiO_2 preexisted at the interface, Si reacts with adsorbed oxygen at the surface to form SiO; (e) SiO desorbes from exposed SiO_2 covered Si through pre-existing pinholes in the high-*k* film (f) similar process as in (e) but assuming that no SiO_2 preexisted at the interface.

Figure 4

Cross-section HRTEM images of ZrO_2 grown be reactive evaporation on Si substrates: (a) the as-deposited stack, (b) after annealing at 1000 ˚C and ~10^{-4} torr, (c) after annealing at 1000 ˚C and ~10^{-5} torr. Micrographs (a) and (b) were recorded from areas of the samples that were covered by the patterned Pt electrode. Figure first published in [10].

Figure 5

Cross-section HRTEM images of ZrO_2 grown be reactive evaporation on silicon substrates after annealing at 1000 ˚C and ~10^{-7} torr. The image was recorded from an area of the sample that was covered by the patterned Pt electrode. Figure first published in [10].

Figure 6

(a) Components of the system for which the thermodynamic analysis in section III (b) is performed. (b) Silicide reaction process after ref. [8]: diffusion of excess Zr from of the oxygen deficient ZrO_{2-x} to the Si interface, reaction of the Zr with Si to $ZrSi_2$, while the remaining ZrO_2 is stoichiometric (see text).

Figure A.1.

TALLAN *et al.*'s experimental data of the deviation of stoichiometry in $HfO_{2+\partial}$ at different temperatures as a function of oxygen partial pressure [43]. The solid lines reflect curve fits according to eqn. (A.3). The data at 1200 ˚C, 1300 ˚C and 1400 ˚C was fit assuming $B = 0$.

Figure 1 (a)-(d)

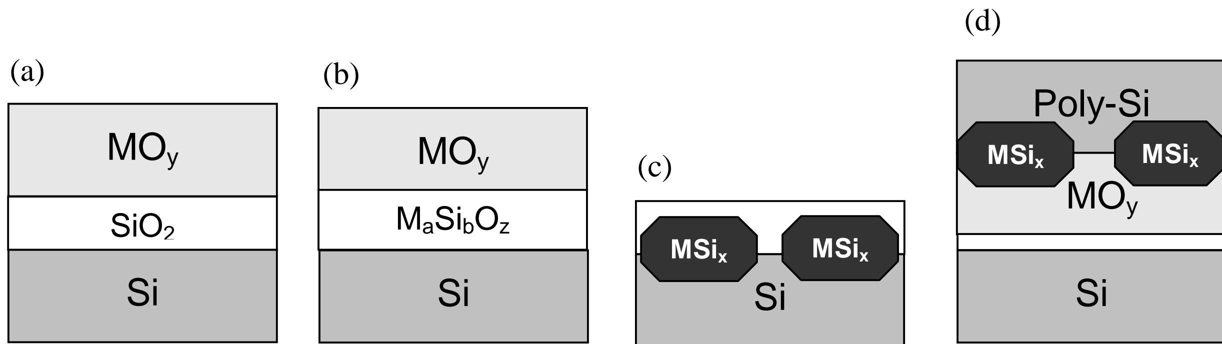

Figure 2

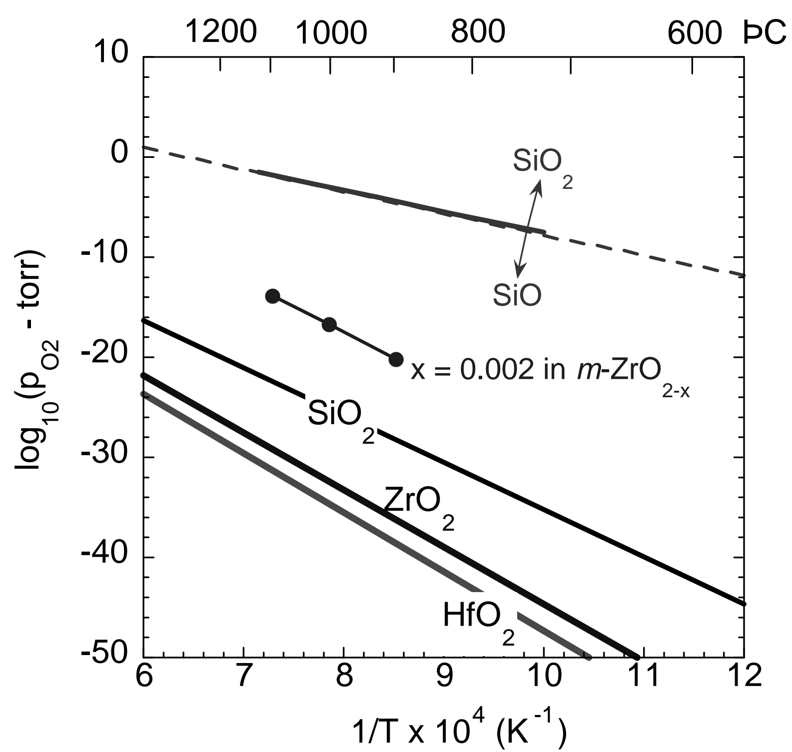

Figure 3 (a)-(f)

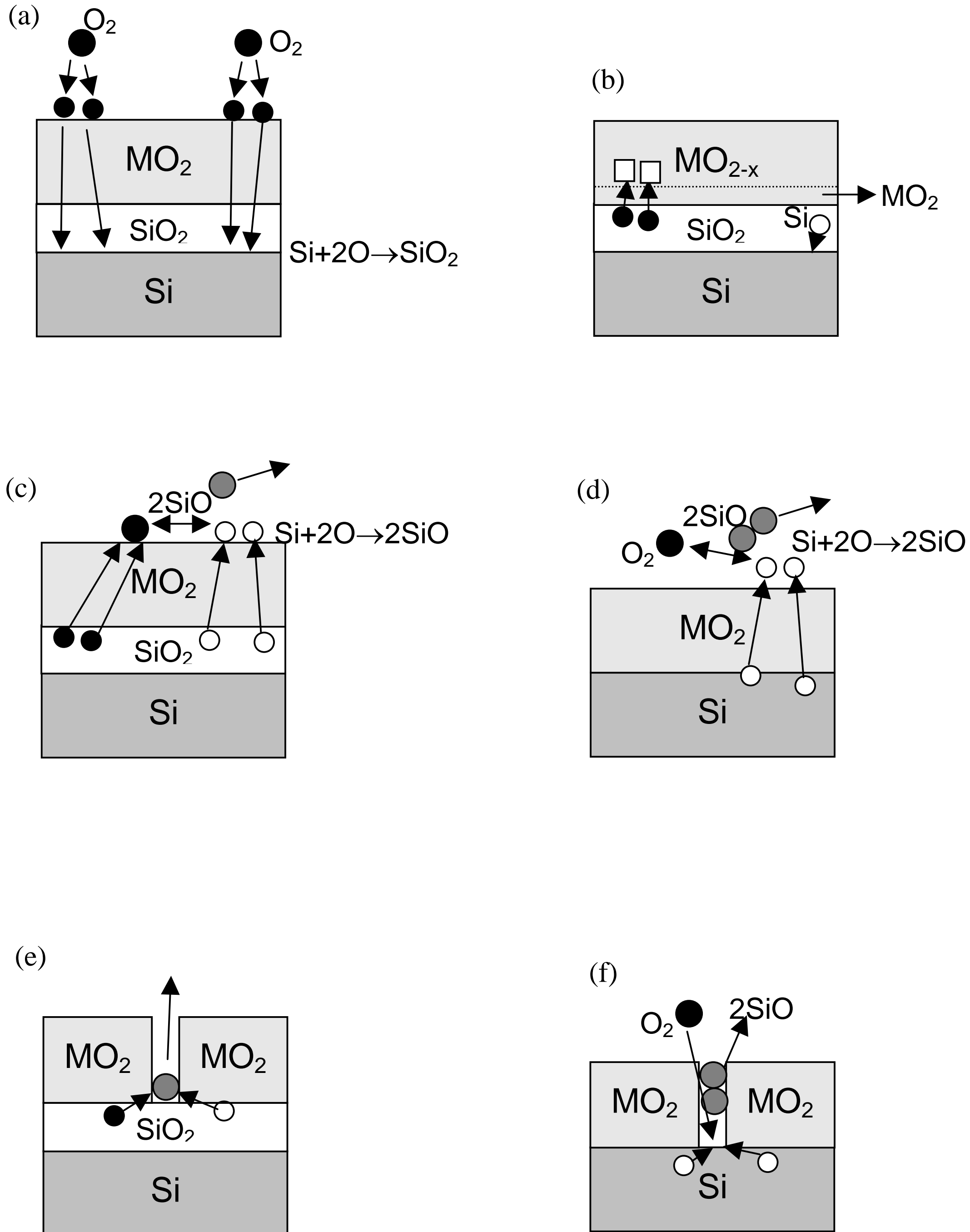

Figure 4

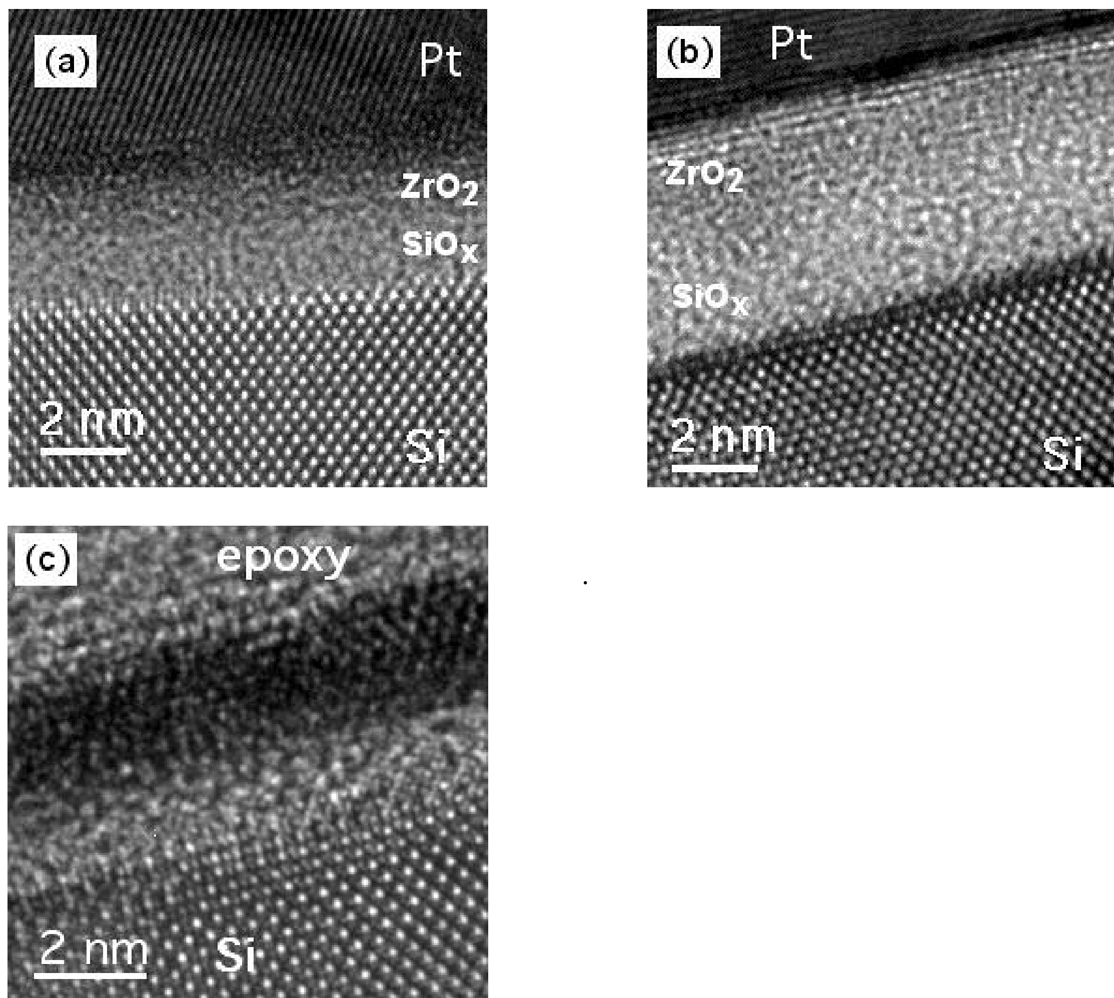

Figure 5

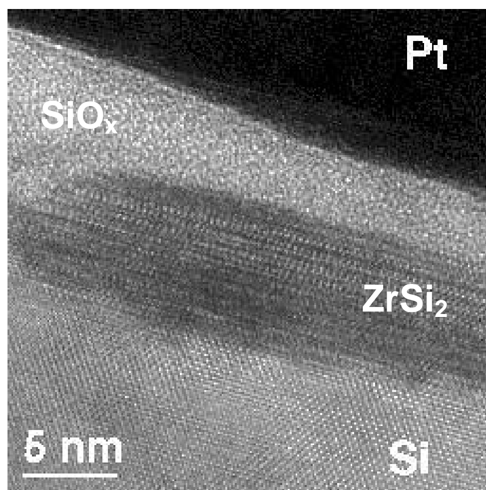

Figure 6

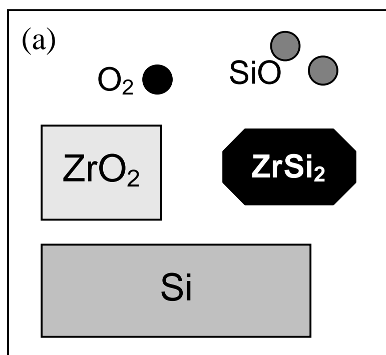

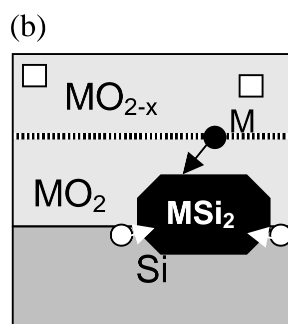

Figure A.1.